ASSESSMENT OF FAILURE MODES IN COMPRESSION LOADED LAMINATES USING QUASI IN SITU COMPUTERIZED TOMOGRAPHY SCANS.

Jonas J. A. D'haen[1], S. Kerscher[1], M. May[2], S. Hiermaier[2]

[1] BMW AG, Hufelandstraße 5, 80788 Munich, Germany, Jonas.Dhaen@bmw.de
[2] Fraunhofer Institute for High-Speed Dynamics, EMI, Eckerstraße 4, 79104 Freiburg, Germany

Keywords: Progressive failure, Computerized tomography, Material characterization, in situ testing

Abstract
From literature it is known that the specific energy absorption of carbon fiber composites surpasses the steel equivalent [1], [2]. However, it should be noted that these values are obtained when the material fails optimally. Material defects, small off axis loadings and wrong damage initiation could lead to a significant lower energy absorption. Therefore, it is important that the material is fully understood to ensure broad adoption in the industry. This research will investigate the failure evolution for a $[45,-45,0]_s$ stacking sequences using sequential computerized tomography scans. It is seen from results that the proposed methodology works well to investigate failure evolution. Furthermore, it is seen that the failure growth is repeatable for specimen with the same layup.

1. Introduction

Damage evolution in composite materials is a complex process, this can be explained from the definition of composite materials. "Composites are made from more or equal to two materials with considerable different properties that are combined to act as one. Such that they react different then the single materials separately." The fact that two materials are interconnected with each other make the initial failure result in triggering a complex interaction between the two materials. The amount of possible failure modes is enormous due to the composition. Also, it should be mentioned that the mechanisms that dominate the failure evolution in composite materials are not fully understood yet [3]. In order to be able to adopt carbon fiber composites in energy absorption structures it is essential that the progressive failure matches the calculated one accuratlly. This research is focused on failure behavior of carbon fiber composites to get a better understanding on the material behavior after first ply failure.
The approach that is selected to investigate the failure modes of the laminate is quasi in situ computerized tomography (CT) scans during various loading states. Literature shows that in situ computerized tomography tests on carbon fiber composites have been performed before. The first paper is published by Wright et al [4], they elaborate on the advantages of this new technique such as identifying damage evolution and visualizing three dimensional strain fields.
Moffat et al [5] write about in situ CT scans of cross ply laminates to investigate three dimensional damage. Furthermore, they concludes that it is possible to investigate the complex shape of 0° splits. Both published another paper in 2010, Moffat et al describe the usage of computerized laminograpy to visualize damage mechanisms in large planar samples that would not have been possible with a CT scan [6]. Wright describes that it is possible to calculate local displacement fields around the intra-laminar 0° split [7]. More relevant literature has been found but is outside the scope of this paper [8]–[12]. Presented literature study tension or impact loading cases whereas this paper will elaborate on

compression loaded multi-directional laminate. The goal of this paper is to get more insights on the damage evolution and failure mode propagation of a multi-directional laminate loaded in compression. The investigated stacking sequence is $[45,-45,0]_S$ loaded in 0° and 90° direction.

2. Test setup

Gathering in situ data requires the computerized tomography machine to perform a scan during testing. For example, by placing a test rig inside a CT machine. Because of practical and financial reasons this was not possible. Therefore, it is chosen to perform the tests and scans consecutively in their own device. Initially, a CT scan is performed to have a reference measurement. Afterwards, the specimen is taken out and installed in the test rig to be loaded to 95% of the maximum load. A new CT scan is performed followed by a new load cycle up to a force drop of 10%. This loading and scanning step is repeated two times ending up with loadcycle number five which is aborted after 2 min. The fact that CT scans take a significant amount of time, it is decided to scan the specimen in relaxed conditions. This has the advangtage that creep in the material does not influence the CT scans and saves us from constructing a complex loading rig. The potential disadvantage is that cracks are not clearly visible because they are closed.

3. Data acquisition

For this research, it is important to determine when failure occurs, this is usually done by measuring the force using a load cell and strain using strain gauges. [13], [14]. However, in order to measure the strain after initial failure it is necessary to measure the strain using another technique. It is known that strain gauges regularly delaminate or break after initial failure, whereas ultimate failure for multi-directional laminates is far from being reached. This results in the fact that strain will be measured using digital image correlation (DIC). From literature it is seen that the side view results in the most consistent results to determine the strain after first ply failure [15]. Reference measurements for the laminate that is investigated in this research are shown in figure 2.

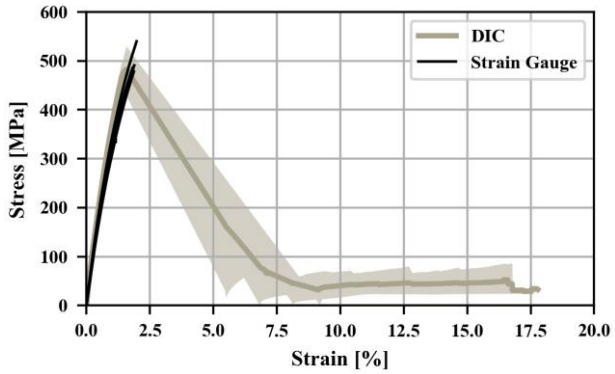

Figure 1. Comparison between DIC and stain gauge data acquisition for a $[45,-45,0]_s$ laminate.

The CT machine used for this work originates from GE and is called “phoenix v|tome|x m”. Each scan consists out of eight specimen to speed up the process. Settings where chosen such that the scan finishes within three hours with a voxel size of 13 µm. Post processing of the data is neccesarry to reconstruct, cut out and match the data with the other loading steps. The matching is done using the feature based registration to make sure that the coordinate systems are consistent.

4. CT Scan results

Results are gathered in two forms, the first is a stress strain curve, the second are CT images where the failure mode in the specimen are analysed. The stress strain images are composed by overlaying the data from the multiple loading sequences. These are compared to reference measurements visualized with a black line as the average and a gray zone span between the minimum and maximum value. Stopping criteria for the points are summarized in the table below, for easy interpretation of the figure.

The results that are obtained for a laminate loaded in 0° are shown in figure 2 and table 1. Only three measuring points are gathered for this load case because it is not possible to perform a CT scan after a force drop of 10%. The force drop happens as an high dynamic process without being able to stop it, although the test being quasi static.

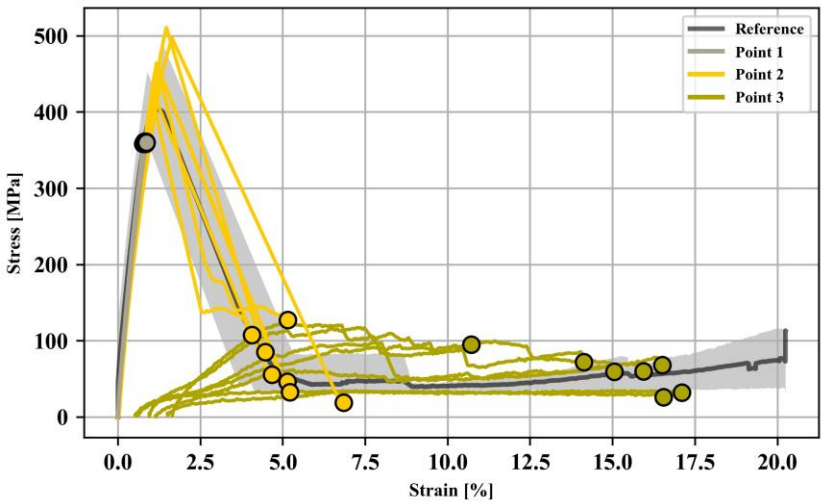

Figure 2. Stress Strain curves of a compression loaded 0° $[45,-45,0]_S$ laminate.

Table 1. Halt criteria for a $[45,-45,0]_S$ specimen loaded in 0°.

Point	Halt criteria
Point 1	95% of the maximum force of the reference measurements
Point 2	After a Force drop of 10 %
Point 3	Two minutes of testing with a speed of 1 mm/min

CT scans that are obtained at the halt points are visualized in figure 3, remember that this is a cross section and therefore not all failure modes are visible in there. Accompanied with this figure is a table that lists all the failure modes that have been observed in the specimen. The visually dominating failure modes are highlighted in bold and the integers listed behind the failure modes repsresent the layer where the failure occurs. The layers are counted from the left to right, in case of failure between two layers, like delamination, this is indicated with a dash between the corresponding layers.

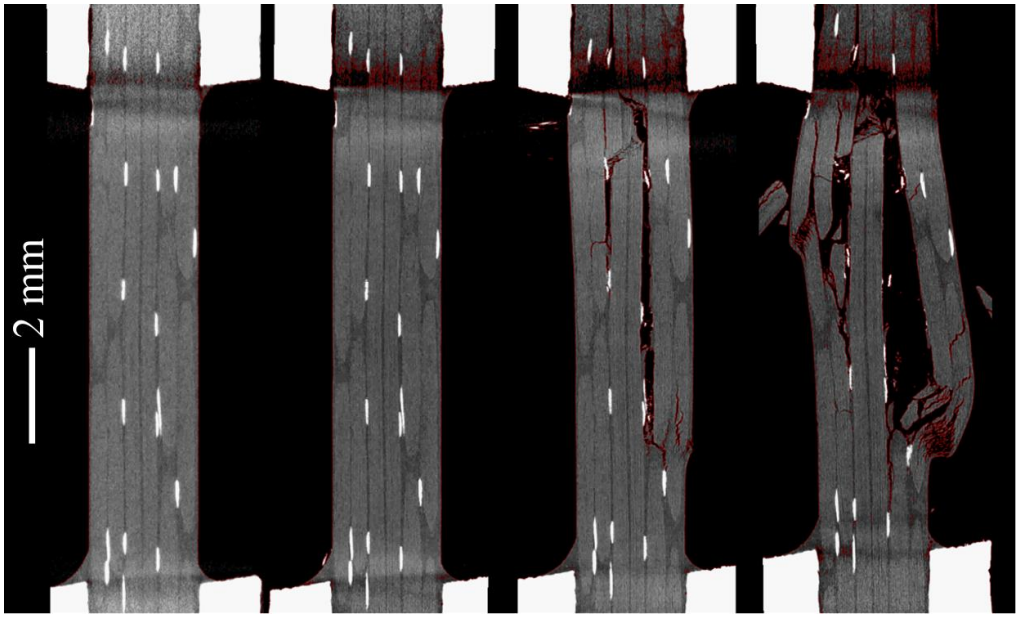

Figure 3. Cross section trough the width of an 0° $[45,-45,0]_s$ laminate. F.l.t.r. Reference measurement, point 1, point 2, point 3.

The white vertical lines visible in the CT scan figures are glass fiber bundels in the material to enhance handling during production. The white pieces on the top and bottom of the specimen are the glass fiber tabs used as force introduction. The third specimen, point 2, shows fiber kinking at the top side of the middle two layers and delamination between layer two and three & four and five. Point 3 shows the same failure modes as point 2 plus a pop up delamination in layer five and six. Furthermore, shear failure is seen observed in layer one, two, five and six. The complete list of failure modes is shown in table 2.

Table 2. Failure modes that occurring inside the laminate.

Point	Failure modes
Point 1	--
Point 2	**Kinking (3,4), Compressive fiber failure (3,4)**, Fiber/matrix debonding (3,4), Delamination (2-3, 4-5), Shear failure (1,2,5,6)
Point 3	Kinking (3,4) Multi Compressive fiber failure (3,4), Fiber/matrix debonding (3,4) **Pop-up delamination(2-3, 4-5) Buckling (1-2,5-6) Shear failure (1,2,5,6)**

The same work is performed in 90° direction. This loading direction has the advantage that the failure happens more gradually, meaning that more measuring points can be obtained during failure evolution. The halt criteria that are used for the 90° direction are presented in table 3.

Table 3. Halt criteria for a $[45,-45,0]_S$ specimen loaded in 90°.

Point	Halt criteria
Point 1	95% of the maximum force of the reference measurements
Point 2	After a Force drop of 10 %
Point 3	After a Force drop of 10 %
Point 4	After a Force drop of 10 %
Point 5	Two minutes of testing with a speed of 1 mm/min

During testing plastic strain accumulates, the plastic strain is calculated by using the same reference frame of a specimen for all measurement points. The resulting stress strain curves from the DIC are shown in Figure 4. Plastic strain can be observed by a horizontal shift to the right of the measurement lines.

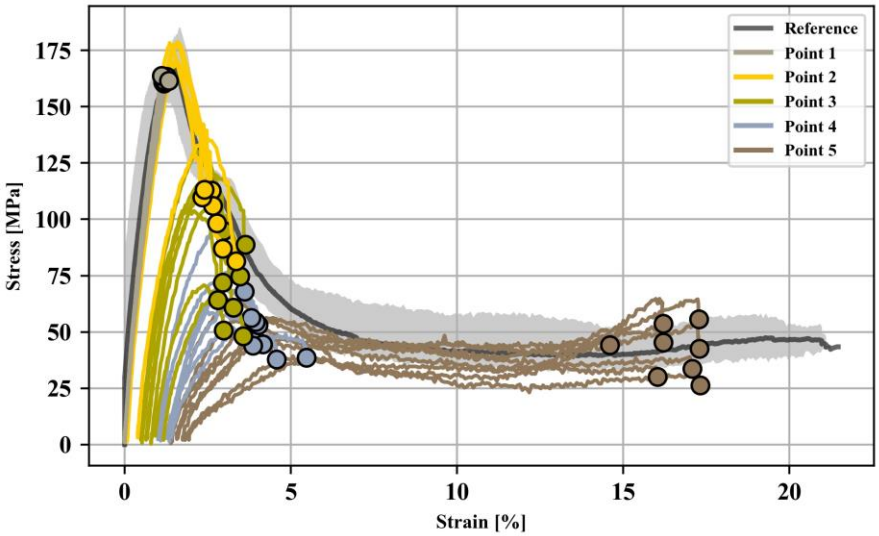

Figure 4. Stress Strain curves of a compression loaded 90° $[45,-45,0]_S$.

The results from the CT scan in 90° direction are shown in figure 5, it can be seen that the failure evolution occurs in a more controled way compared to the 0° variant. Initial failure in point 2 shows delamination between layer two and three. For point 3 an additional shear failure occurs in the two middle layers. Additionally shear failure is seen in layers one, two, five and six for point 4, wheres complete failure is seen in point 5. Table 4 Lists all the failure modes that have been observed in the specimen.

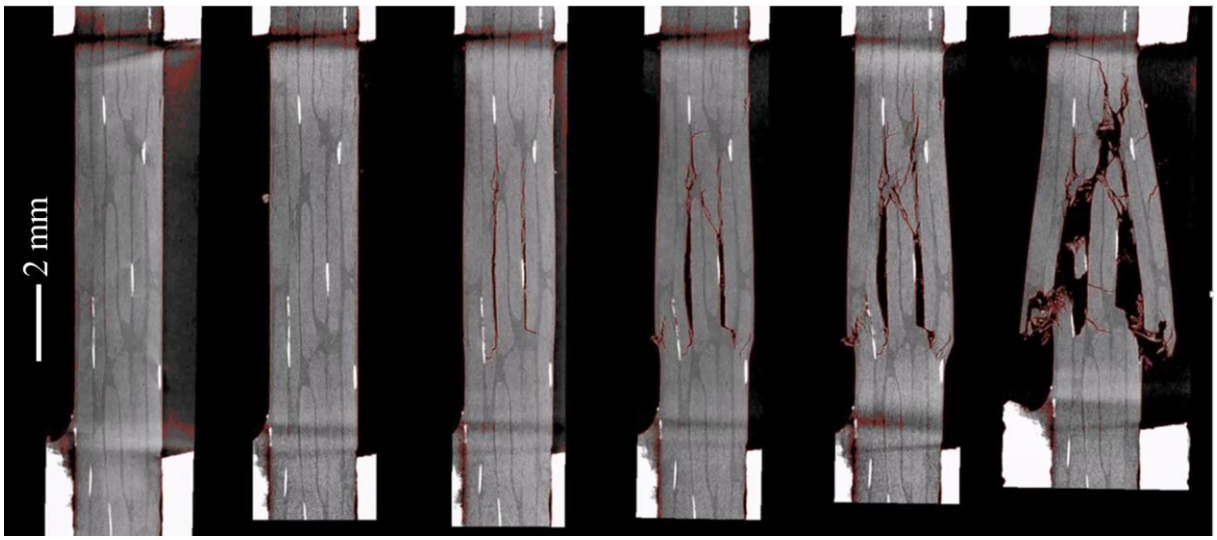

Figure 5. Cross section trough the width of an 0° $[45,-45,0]_s$ laminate. F.l.t.r. Reference measurement, point 1, point 2, point 3, point 4, point 5.

Table 4. Failure modes that occurring inside the laminate.

Point	Failure modes
Point 1	--
Point 2	**Delamination (2-3,4-5),** Shear failure (2,5), Kinking + shear failure (1,6)
Point 3	**Delamination (2-3,4-5), Shear failure (3-4),** Shear failure (1,2,5,6) Kinking + shear failure (1,6)
Point 4	**Delamination (2-3,4-5), Shear failure (3-4),** Shear failure (1,2,5,6), Kinking + shear failure (1,6)
Point 5	Delamination (2-3,4-5), **Shear failure (3-4), Shear failure (1,2,5,6)**

5. Conclusion & recommendation

Previous sections give insight in how quasi in situ CT scans for compression loaded specimen can be performed. The results that are discussed in section 4 show that discontinuous testing results match with the behavior of reference measurements. Furthermore, it is seen that the specimens degrade at the same point with the same slide, from this it can be expected that the damage evolution inside the specimen occurs repeatable. This fact is also observed in the CT scan data.
A recommendation for following research is to perform real in situ tests and therefor avoid scanning relaxed specimens, this way it could be assumed that no closed cracks are present. This would prevent adjusting the coordinate system for every CT scans.

As an outlook for follow-up work; outcomes from this work will be set side by side to a high detailed finite element simulation. Failure modes and stress strain curves will be compared in order to verify the accuracy and capabilities of detailed finite element simulations. The gained knowledge from this comparison can then be used as guidelines for future development projects.

Acknowledgments

The author thanks BMW AG, Fraunhofer Institute for High-Speed Dynamics and Albert Ludwig University of Freiburg for the generous support.

References

[1] G. L. Farley, “Energy Absorption of Composite Materials,” *J. Compos. Mater.*, vol. 17, no. 3, pp. 267–279, 1983.
[2] J.J. Carruthers, A. P. Kettle, and A. M. Robinson, “Energy absorption capability and crashworthiness of composite material structures : A review,” *Appl. Mech. Rev.*, vol. 51, no. 10, pp. 635–649, 2015.
[3] S. T. Pinho, L. Iannucci, and P. Robinson, “Physically based failure models and criteria for laminated fibre-reinforced composites with emphasis on fibre kinking. Part II: FE implementation,” *Compos. Part A*, vol. 37, no. 5, pp. 766–777, 2006.
[4] P. Wright, X. Fu, I. Sinclair, and S. M. Spearing, “Ultra High Resolution Computed Tomography of Damage in Notched Carbon Fiber—Epoxy Composites,” *J. Compos. Mater.*, vol. 42, no. 19, pp. 1993–2002, Oct. 2008.
[5] A. J. Moffat, P. Wright, J.-Y. Buffière, I. Sinclair, and S. M. Spearing, “Micromechanisms of damage in 0° splits in a [90/0]s composite material using synchrotron radiation computed tomography,” *Scr. Mater.*, vol. 59, no. 10, pp. 1043–1046, Nov. 2008.

[6] A. J. Moffat *et al.*, “In situ synchrotron computed laminography of damage in carbon fibre–epoxy [90/0]s laminates,” *Scr. Mater.*, vol. 62, no. 2, pp. 97–100, Jan. 2010.
[7] P. Wright, A. Moffat, I. Sinclair, and S. M. Spearing, “High resolution tomographic imaging and modelling of notch tip damage in a laminated composite,” *Compos. Sci. Technol.*, vol. 70, no. 10, pp. 1444–1452, Sep. 2010.
[8] A. E. Scott, M. Mavrogordato, P. Wright, I. Sinclair, and S. M. Spearing, “In situ fibre fracture measurement in carbon–epoxy laminates using high resolution computed tomography,” *Compos. Sci. Technol.*, vol. 71, no. 12, pp. 1471–1477, Aug. 2011.
[9] A. E. Scott, I. Sinclair, S. M. Spearing, A. Thionnet, and A. R. Bunsell, “Damage accumulation in a carbon/epoxy composite: Comparison between a multiscale model and computed tomography experimental results,” *Compos. Part Appl. Sci. Manuf.*, vol. 43, no. 9, pp. 1514–1522, Sep. 2012.
[10] D. J. Bull, L. Helfen, I. Sinclair, S. M. Spearing, and T. Baumbach, “A comparison of multi-scale 3D X-ray tomographic inspection techniques for assessing carbon fibre composite impact damage,” *Compos. Sci. Technol.*, vol. 75, pp. 55–61, 2013.
[11] D. J. Bull, A. E. Scott, S. M. Spearing, and I. Sinclair, “The influence of toughening-particles in CFRPs on low velocity impact damage resistance performance,” *Compos. Part Appl. Sci. Manuf.*, vol. 58, pp. 47–55, 2014.
[12] Y. Swolfs *et al.*, “Synchrotron radiation computed tomography for experimental validation of a tensile strength model for unidirectional fibre-reinforced composites,” *Compos. Part Appl. Sci. Manuf.*, vol. 77, pp. 106–113, Oct. 2015.
[13] DIN Deutsches Institut für Normung e. V., “DIN EN ISO 14126-99: Bestimmung der Druckeigenschaften in der Laminatebene,” vol. 2000, 2000.
[14] ASTM Standard, “D6641-09: Standard Test Method for Compressive Properties of Polymer Matrix Composite Materials Using a Combined Loading Compression Test Fixture,” 2009.
[15] J. J. A. D’haen, S. Kilchert, O. Knoll, M. May, and S. Hiermaier, “Progressive failure strain measurement of a compression loaded carbon fiber laminate,” in *ICCM21*, 2017, pp. 1–7.